

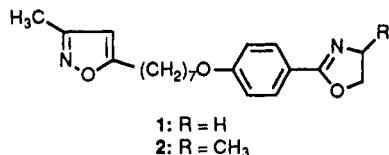
# CoMFA Analysis of the Interactions of Antipicornavirus Compounds in the Binding Pocket of Human Rhinovirus-14

Guy D. Diana,\* Paul Kowalczyk, Adi M. Treasurywala, Richard C. Oglesby, Daniel C. Pevear, and Frank J. Dutko

Sterling Winthrop Pharmaceuticals Research Division, Rensselaer, New York 12144. Received June 14, 1991

A CoMFA analysis of eight compounds related to disoxaril whose X-ray structures bound to HRV-14 had been determined resulted in a strong positive correlation of activity with steric effects of the compounds, particularly toward the pore end of the compound binding site, and no correlation with electrostatic effects. These results confirm what had been previously found, that the activity of these compounds was highly dependent upon their hydrophobic nature as expressed by log *p*. The CoMFA study also confirmed the results from the comparison of a series of active and inactive compounds using volume maps which showed that bulk at the pore end of the molecule was conducive to high levels of antiviral activity while excessive bulk around the ring led to poor activity.

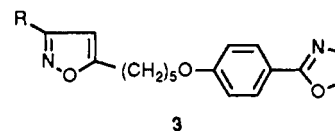
Since the determination of the three-dimensional structure of human rhinovirus-14<sup>1</sup> (HRV-14) and the subsequent elucidation of the binding site of disoxaril 1



and the 4-methyloxazol-5-yl homologue 2,<sup>2</sup> there has been interest in our laboratories in understanding the molecular interaction between the protein coat of HRV-14 and several analogues of these compounds in an effort to utilize this information in the design of more potent antipicornaviral agents. Our initial efforts in this regard were focused on examining the enantiomeric specificity of binding for various substituents on the oxazoline ring of this family of compounds. The results of this study could be explained on the basis of steric effects alone and this finding pointed to the conclusion that steric or van der Waals' interactions between the pocket and the drugs were the determining factor for biological activity.<sup>3a</sup> This result has been reinforced through the design, synthesis, and evaluation of new molecules.

An analysis of a series of active and inactive analogues using simple volume maps and utilizing the active analogue

approach demonstrated that steric fit could be used to rationalize the majority of the data accumulated at this time.<sup>3b</sup> These volume maps remain a useful abstraction of the data from X-ray analysis of a series of disoxaril analogues bound to HRV-14. It was found that excessive bulk<sup>4</sup> on the phenyl ring resulted in inactive compounds while compounds with bulky groups attached to the isoxazole ring exhibited enhanced activity. Subsequently, a series of extended chain homologues 3 was synthesized



and tested against HRV-14. Increasing the size of the chain R from methyl to propyl resulted in a concomitant increase in activity which supported the conclusions drawn from this study. Although the exact conformation of the side chains of these compounds when bound to HRV-14 was unknown, we assumed, based on previous studies, that the side chains were extended into the "pore" area of the compound binding site (Figure 1).

The studies previously described dealt with the effect of the hydrophobicity of this series of compounds on activity, exclusive of any electrostatic effects. In view of the structure-activity studies which we had performed on analogues with a variety of substituents on the phenyl ring,<sup>3c,d</sup> we were interested in examining the effects of these substituents on the binding to HRV-14 and on the activity against this serotype.

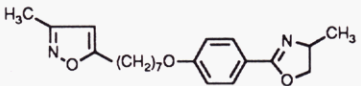
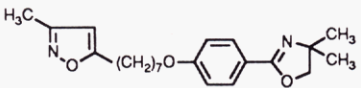
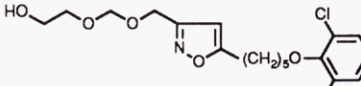
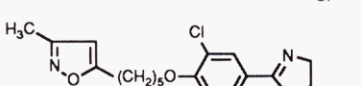
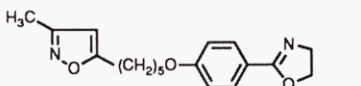
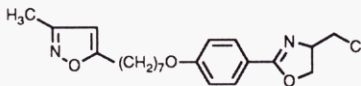
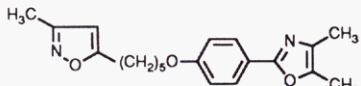
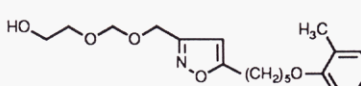
One of the early results which emerged from the X-ray analysis showed that the orientational preference in each case examined was not the same for all the drugs.<sup>5</sup> Some compounds appeared to prefer binding with the isoxazole at the so-called "heel" of the pocket, whereas other analogues preferred binding in the opposite orientation, i.e. with the isoxazole ring in the "toe" (Figure 1). If, however, this binding preference were unknown, it could complicate any SAR analysis based on assumed orientations of any molecule in the pocket (and consequently on the developing volume maps). This type of sensitive orientational dependence has been reported in the case of the dihydrofolate reductase inhibitor trimethoprim.<sup>6,7</sup> Here the

- (1) Rossmann, M. J.; Arnold, E.; Erickson, J. W.; Frankenberger, E. A.; Griffith, J. P.; Hecht, H. J.; Johnson, J. E.; Kramer, G.; Luo, M.; Mosser, A. G.; Reuckert, R. R.; Sherry, B.; Vriend, G. Structure of a Human Common Cold Virus and Functional Relationship to Other Picornaviruses. *Nature* 1985, 317, 145-153.
- (2) Smith, T. J.; Kremer, M. J.; Luo, M.; Vriend, G.; Arnold, E.; Kramer, G.; Rossmann, M. G.; McKinlay, M. A.; Diana, G. D.; Otto, M. G. The Site of Attachment in Human Rhinovirus 14 for Antiviral Agents that Inhibit Uncoating. *Science* 1986, 233, 1286-1291.
- (3) (a) Diana, G. D.; Otto, M. J.; Treasurywala, A. M.; McKinlay, M. A.; Oglesby, R. C.; Maliski, E. D.; Rossmann, M. G.; Smith, T. J. Enantiomeric Effects of Homologues of Disoxaril on the Inhibitory Activity of Human Rhinovirus-14. *J. Med. Chem.* 1988, 31, 540-544. (b) Diana, G. D.; Treasurywala, A. M.; Bailey, T. R.; Oglesby, R. C.; Pevear, D. C.; Dutko, F. J. A Model for Compounds Active against Human Rhinovirus-14 Based on X-ray Crystallography data. *J. Med. Chem.* 1990, 33, 1306-1311. (c) Diana, G. D.; Oglesby, R. C.; Akullian, V.; Carabateas, P. M.; Cutcliffe, D.; Mallamo, J. P.; Otto, M. J.; McKinlay, M. A.; Maliski, E. G.; Michalec, S. J. Structure-Activity Studies of 5-[[4-(4,4-Dihydro-2-oxazolyl)phenoxy]alkyl]-3-methylisoxazoles: Inhibitors of Picornavirus Uncoating. *J. Med. Chem.* 1987, 30, 383-386. (d) Diana, G. D.; Cutcliffe, D.; Oglesby, R. C.; Otto, M. J.; Mallamo, J. P.; Akullian, V.; McKinlay, M. A. Synthesis and Structure-Activity Studies of Some Disubstituted Phenylisoxazoles against Human Picornaviruses. *J. Med. Chem.* 1989, 32, 450-455.

(4) The terms "bulk" and "hydrophobicity" will be used interchangeably in this paper and refer to entropic properties of the molecules.

(5) Badger, J.; Minor, I.; Kremer, M. J.; Oliveria, M. A.; Smith, T. J.; Griffith, J. P.; Guerin, D. M.; Krishnaswamy, S.; Luo, M.; Rossmann, M. J.; McKinlay, M. A.; Diana, G. D.; Dutko, F. J.; Fancher, M.; Reuckert, R. R.; Heinz, B. A. Structural Analysis of a Series of Antiviral Agents Complexed with Human Rhinovirus 14. *Proc. Natl. Acad. Sci. U.S.A.* 1988, 85, 3304-3308.

Table I. Inhibitory Effect against HRV-14

compd no.		MIC ( $\mu$ M) HRV-14
5 <sup>a</sup>		0.05
6 <sup>a</sup>		0.16
7 <sup>b</sup>		0.06
4 <sup>c</sup>		2.41
8 <sup>a</sup>		0.51
9 <sup>d</sup>		0.03
10 <sup>b</sup>		0.14
11		0.06

<sup>a</sup> See ref 9. <sup>b</sup> See ref 3b. <sup>c</sup> See ref 3a. <sup>d</sup> See ref 3d.

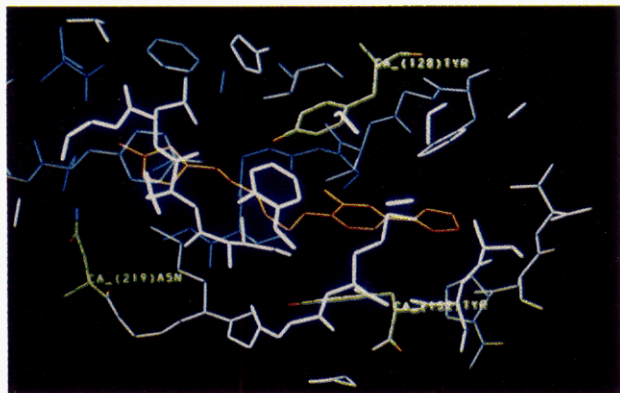


**Figure 1.** Compound 4 (orange), bound to the hydrophobic binding site of HRV-14 obtained from X-ray crystallography studies by J. Badger et al., Purdue University.

expected orientation was shown to be incorrect by an X-ray analysis of both the substrate and the inhibitor bound to the active site.

One of the compounds studied, 4 (Table I), lay deep within a hydrophobic pocket in one of the viral proteins, VP<sub>1</sub>, comprising the capsid protein (Figure 1), with the

isoxazole end of the molecule residing below the pore leading to the "canyon" or putative cell receptor binding site. The phenyl ring of this compound appeared to be in a stacking configuration with respect to Tyr<sup>128</sup> and Tyr<sup>152</sup> (Figure 2). The chlorine on the aromatic ring could impart an electronic effect, and consequently, it was assumed that the electronics at this end of the molecule might influence the extent of stacking. To explore this possibility we examined several compounds related to 4, shown in Table I, using the program CoMFA (comparative molecular field analysis).<sup>8,10</sup> Since the conclusions with regard to orientation of the antipicornavirus compounds were based on X-ray crystallography studies, failures ascribed to the erroneous choice of biorelevant conformations or orientations were not an issue.

## Chemistry

The synthesis of compounds 5–10 in Table I was previously reported.<sup>3b,c</sup> The synthesis of compound 11 is shown in Scheme I. 3,5-Dimethyl-4-hydroxybenzonitrile was alkylated with 5-(5-chloropentyl)-3-(hydroxymethyl)isoxazole<sup>3b</sup> (12) in DMF to give 14 in 79% yield. Treatment of 14 with sodium azide in DMF provided tetrazole 15 in 78% yield. Alkylation of 15 with methyl iodide and potassium carbonate in acetonitrile gave a 70/30 mixture of 16 and the regioisomer. This mixture was separated by MPLC and compound 16 was isolated in 59% yield. The isomers were characterized by the differences in the chemical shifts of the aromatic protons adjacent to the tetrazole ring ( $\delta$  7.79 and 7.38, respectively) as well as the methyl protons at  $\delta$  4.36 and 4.16. In ad-

- (6) Bolin, J. T.; Filman, D. J.; Mathews, D. A.; Hamlin, R. C.; Kraut, J. Crystal Structure of Escherichia Coli and Lactobacillus Casei Dihydrofolate Reductase at 1.7Å Resolution I. General Features and Binding of Methotrexate. *J. Biol. Chem.* **1982**, *257*, 13650–13662.
- (7) Filman, D. J.; Bolin, J. T.; Mathews, D. A.; Kraut, J. Crystal Structure of Escherichia Coli and Lactobacillus Casei Dihydrofolate Reductase at 1.7Å Resolution II. Environment of Bound NADPH and Implications for Catalysis. *J. Biol. Chem.* **1982**, *257*, 13663–13672.

- (8) Sybyl Molecular Modeling Software, Tripos Associates Inc., St Louis, MO.

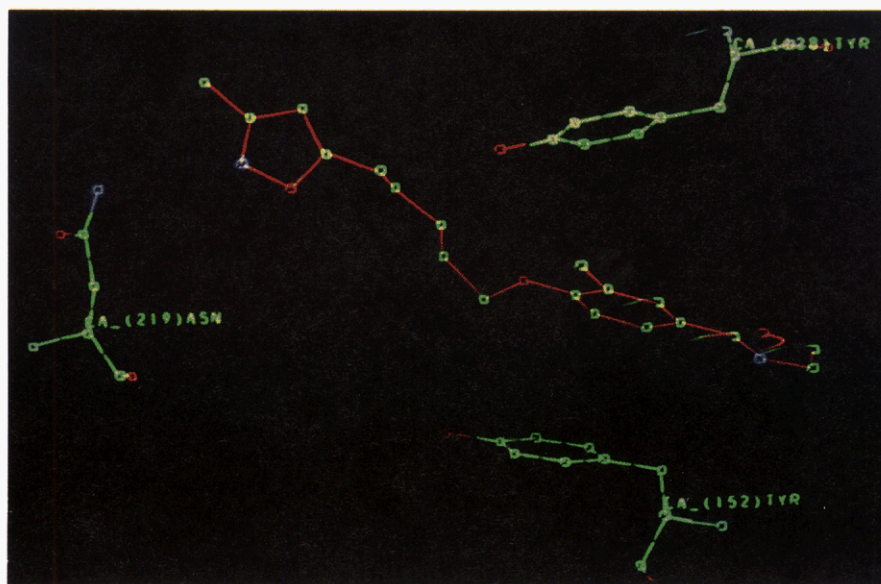


**Figure 2.** Stacking conformation of the phenyl ring of **4** with Tyr<sup>128</sup> and Tyr<sup>152</sup>. Asn<sup>219</sup> residues are at the pore end of the binding site.

**Scheme I**

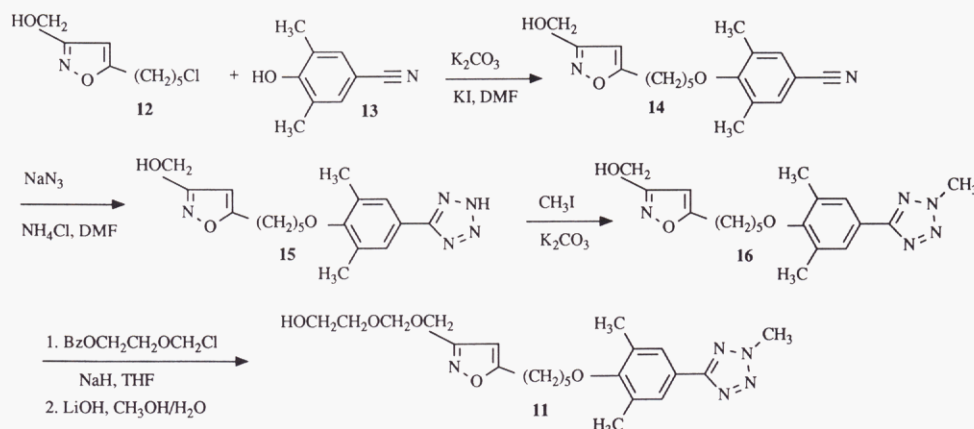


**Table II.** CoMFA<sup>d</sup> Coordinates

no.	MIC <sup>a</sup>	log (1/MIC)	log <i>p</i>	CMR <sup>b</sup>	XDIP <sup>c</sup>	YDIP	ZDIP	DIP
4	2.41	-0.38	4.32	9.340	0.58	-2.78	-5.13	5.86
5	0.05	1.25	5.49	9.313	0.38	3.17	2.43	4.01
6	0.16	0.79	6.20	9.770	0.28	3.22	2.48	4.08
7	0.06	1.20	3.07	12.146	4.80	2.04	-2.70	5.88
8	0.51	0.14	3.90	8.849	0.10	-1.36	-3.82	4.05
9	0.03	1.47	6.02	10.268	1.15	0.98	1.61	2.20
10	0.14	0.85	6.11	10.175	0.18	-0.38	-3.26	3.29
11	0.06	1.23	2.26	12.152	3.92	3.68	-1.87	5.69

<sup>a</sup> Minimum inhibitory concentration against HRV-14. <sup>b</sup> Molar refractivity. <sup>c</sup> Dipole moments. Atomic point charges were calculated using MOPAC version 5.0<sup>16</sup> with the AM1 Hamiltonian.<sup>11</sup> <sup>d</sup> CoMFA generated data using a hydrogen ion probe. Partial least squares was used for analysis of data employing five cross-validation groups, three components, and 100 iterations. Cross-validation  $R^2 = 0.728$ .

dition, X-ray crystallography studies supported the structural assignments. Compound **11** was prepared in 51% from **16** by alkylation with 2-(chloromethoxy)ethylbenzoate<sup>9</sup> followed by hydrolysis of the benzoate ester with lithium hydroxide.

#### QSAR Table

The choice of compounds in Table I was based on the availability of crystallographic data of the compound bound in the pocket of HRV-14. No attempt was made

to select these compounds based on any other criterion. This gave a reasonable spread of substituents at various locations on the parent structure and coincidentally also provided a reasonable spread of activities. The activity of each of these compounds was determined from a plaque-reduction assay.<sup>11</sup> Van der Waal's radii for the atoms were taken from a standard Tripos force field.<sup>8,12</sup> Charges

(9) Beauchamp, L. M.; Dolmatch, B. L.; Schaeffer, H. J.; Collins, P.; Bayer, D. J.; Keller, P. M.; Fyfe, J. A. Modifications on the Heterocyclic Base of Acyclovir: Synthesis and Antiviral Properties. *J. Med. Chem.* **1985**, *28*, 982-987.

(10) Cramer, R. D., III; Patterson, D. E.; Jeffrey, D. B. Comparative Field Analysis (CoMFA). 1. Effect of Shape on Binding of Steroids to Carrier Proteins. *J. Am. Chem. Soc.* **1988**, *110*, 5959-5967.

(11) Diana, G. D.; McKinlay, M. A.; Brisson, C. J.; Zalay, E. S.; Miralles, J. V.; Salvador, U. J. Isoxazoles with Antipicornavirus Activity. *J. Med. Chem.* **1985**, *28*, 1906-1910.



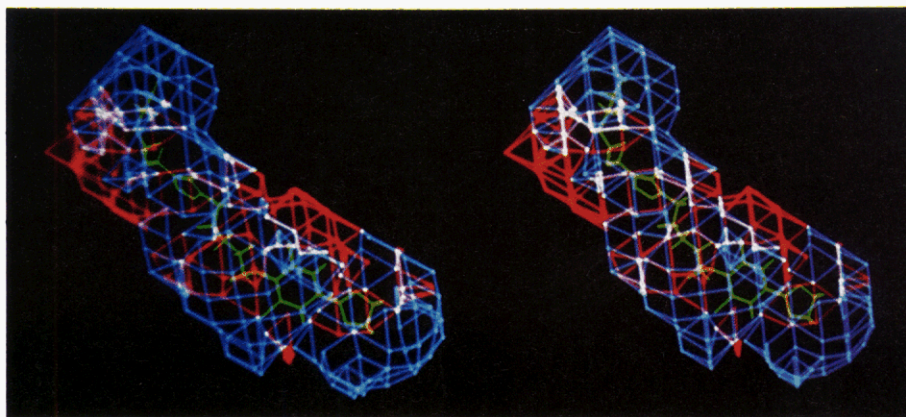


**Figure 3.** Three-dimensional contour map generated from CoMFA analysis of the steric field. The area in blue is indicative of a strong positive correlation with the MIC against HRV-14 while the red area is suggestive of a negative correlation. The grid map is a result of an analysis using a probe atom (charge of 0). All charges on the molecules were calculated using the AM1 Hamiltonian without geometry optimization.

**Table III.** Regression Equation

$$\log (1/\text{MIC}) = 0.349 + ()\log p + ()\text{CMR} + ()\text{XDIP} + ()\text{YDIP} + ()\text{ZDIP} - ()\text{Total DIP}$$

relative contributions	norm. coeff	fraction
$\log p$	0.00032	0.000136
CMR	0.000213	$9.07 \times 10^{-5}$
XDIP	0.000367	0.000156
YDIP	0.001	0.000293
ZDIP	0.001	0.001
total DIP	0.001	0.000283
COMF2 (1755 vars) (steric)	2.170	0.922
COMF2 (1755 vars) (electrostatic)	0.179	0.076

were calculated by the AM1 method<sup>13</sup> by single-point calculations on the receptor-bound conformation of the drug molecule. Point charges on the hydrogen atoms were not collapsed onto the atom to which they were bound but were left on the hydrogen atoms.  $\log p$  values were measured using the shake flask method for partition between octanol and water. Molar refractivities were calculated using the MedChem software package (version 3.54). These physical parameters were all used in the QSAR analysis together with the CoMFA field values which are tabulated in Table II. The CoMFA field values represent several hundred columns for each compound and have been generically displayed as an asterisk. The details of the CoMFA grid and the calculations are included in the Experimental Section.

## Results

The comparative molecular field analysis was carried out in several ways.<sup>10</sup> First, both steric and electrostatic effects were calculated at each of the grid points using a hydrogen atom and a proton respectively as a probe. Cross-validation of the data in Table II using partial least squares (PLS) resulted in a good correlation of MIC with CoMFA data, ( $R^2 = 0.728$ ), with good predictive capabilities in the case of steric properties. However, no substantial correlation was seen with electrostatic parameters either taken in combination with steric factors or considered alone in

**Table IV.** Column Univariate Statics

parameter	mean	minimum	maximum	SD
$\log p$	4.671	2.260	6.200	1.512
CMR	10.252	8.849	12.152	1.260
XDIP	1.428	0.099	4.813	1.859
YDIP	1.082	-2.781	3.696	2.384
ZDIP	-1.280	-5.129	2.487	3.020
total DIP	4.389	2.211	5.886	1.333

**Table V.** Predicted Values of  $\log (1/\text{MIC})$  and Residuals for Compounds in Table I Using the Equation in Table III

compd	actual	calculated	residual
4	-0.38	-0.35	-0.03
5	1.25	1.14	0.11
6	0.79	0.81	-0.02
7	1.20	1.18	0.02
8	0.14	0.13	0.0028
9	1.47	1.56	-0.09
10	0.85	0.84	0.01
11	1.23	1.24	-0.01

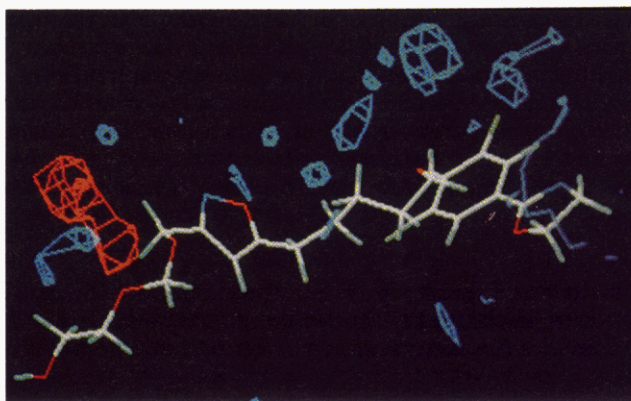


**Figure 4.** Three-dimensional contour map from the analysis of electrostatic fields, showing no correlation with antiviral activity.

a separate CoMFA analysis. A regression equation using all of the values in Table II is shown in Table III. There is essentially no contribution of any of the parameters shown, with the exception of the CoMFA parameters, to the activity of these compounds. Column univariate statistics are listed in Table IV and predicted values and residuals are shown in Table V.

A three-dimensional contour map was generated for both the steric and electrostatic fields (Figures 3 and 4) with compound 7 inserted. It is noteworthy to point out that the electrostatic grid is contoured at 1000 times the sen-

- (12) Vinter, J. G.; Davis, A.; Saunderson, M. R. Strategic Approaches to Drug Design. I. An Integrated Software Framework for Molecular Modelling. *J. Comput.-Aided Mol. Des.* **1987**, *1*, 31-35.
- (13) Dewar, M. J. S.; Zoebisch, E. G.; Healy, J. J. P. Development and Use of Quantum Mechanical Molecular Models. 76.AM1: A New General Purpose Quantum Mechanical Molecular Model. *J. Am. Chem. Soc.* **1985**, *107*, 3902-3909.



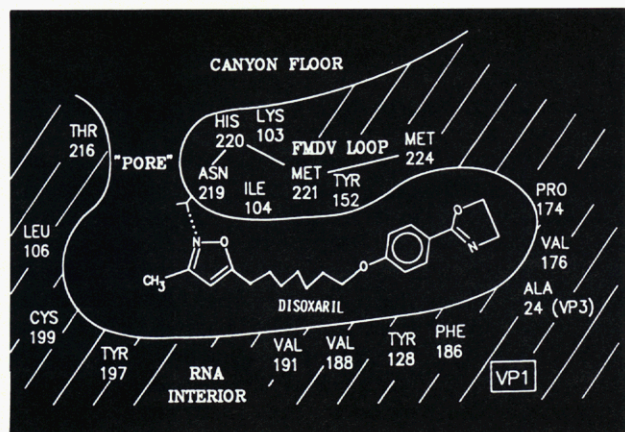


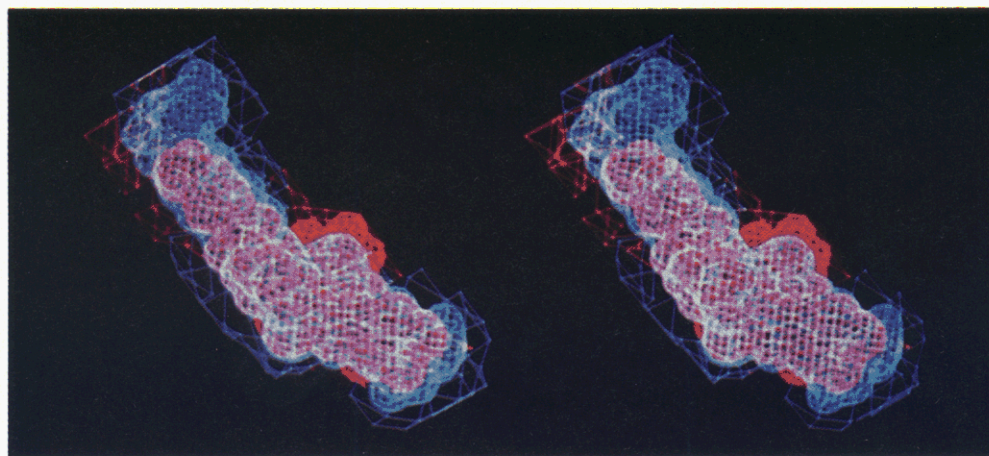
**Figure 5.** Schematic of the compound-binding site in HRV-14. The canyon area is the location of the cell receptor binding site.

sitivity of the steric one. Cutoffs were used to contour together points where the correlations were highest and positive in nature (blue) and those where they were highest and negative in nature (red). Several observations can be made from these maps. First, they qualitatively agree with what is known about the pocket from direct observations. It is important to note that the structure of the macromolecules was not part of the calculations. Thus this agreement tends to bear out the power of this technique to ascertain three-dimensional information that was not

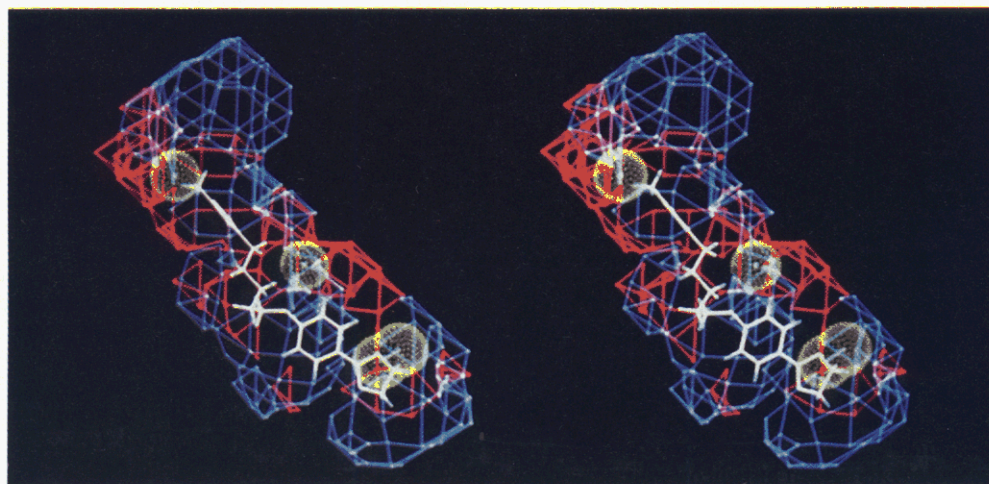
supplied to it at the outset. In agreement with previous attempts and with our knowledge of the residues lining the HRV-14 pocket, this method found no significant correlations between electrostatics and biological activity anywhere around the drug molecules.

A strong association exists (blue) between the steric fields as predicted by the QSAR results and activity and the most significant effect occurs at the pore end of the compound binding site in HRV-14 (Figure 5). Although a moderate positive effect is seen in the vicinity of the aromatic ring, in general, this model predicts that excessive bulk in the aromatic region correlates negatively (red) with activity. These results are in agreement with a related study using volume maps<sup>3b</sup> (Figure 6). The insertion of the CoMFA contour map into the HRV-14 pocket is shown in Figure 7. Only residues within 3 Å of compound 8 are shown by dot surfaces, and it is interesting to note that all of these residues reside within the red area where steric interactions would be predicted to contribute negatively to activity. In contrast to the steric map, the electrostatic map obtained from CoMFA suggests no correlation with MIC (Figure 4).

One of the most striking examples illustrating the effect of bulk on activity at the pore end of the molecule is shown in Table VI. A 20-fold increase in activity was observed by replacing the methyl group of compound 17<sup>3d</sup> with the hydroxylated side chain (7). X-ray crystallography of compound 7 revealed that the side chain is coiled inside the pore rather than being extended, maximizing the hy-

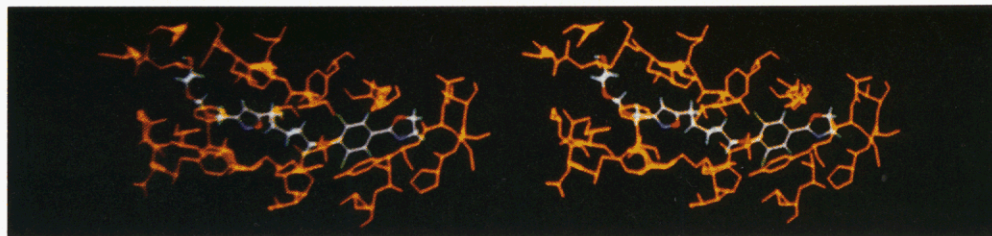


**Figure 6.** An overlay of the volume map generated from a series of active and inactive compounds<sup>3b</sup> and the steric CoMFA map. The blue areas represent a positive correlation with antiviral activity.



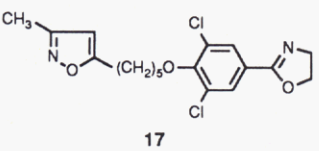
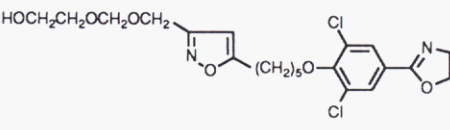
**Figure 7.** CoMFA steric contour map containing compound 8 inserted into the compound-binding site of HRV-14 showing the overlap of the negative contours (red) with several residues which are within 3 Å of 8.





**Figure 8.** Compound 7 bound to VP<sub>1</sub>. The hydroxylated side chain extends upward into the pore in a coiled conformation. The residues are within an 8-Å window.

**Table VI.** A Comparison of Compound 7 and 17 against HRV-14

	HRV-14 (μmol)
 <p>17</p>	1.5
 <p>7</p>	0.09

drophobic interactions with the residues in the pore (Figure 8).

## Discussion

The CoMFA method has proven to be a useful and viable means of correlating properties of biopolymeric host macromolecules with biological activity. In this particular instance, it not only examined the effect of bulk on activity, substantiating the results of the volume map study, but also examined electrostatic effects demonstrating a lack of correlation with antiviral activity. What was particularly required in this study was good structural data with regard to biorelevant conformations and orientations, which was available from X-ray crystallography. The CoMFA study has clearly shown that substituents on the phenyl ring affect activity by virtue of the extent of their hydrophobicity. We have previously shown that some bulk around the phenyl ring is tolerated and desirable but excessive bulk causes a drastic reduction in activity. These results confirm the conclusion drawn from QSAR studies on mono- and disubstituted analogues where a good correlation was observed between log *p* and activity.<sup>3c,d</sup> In the case of the monosubstituted compounds, there was a positive contribution from substituents on the phenyl ring whereas a negative effect was observed from these substituents in the disubstituted series, probably due to spacial constraints within the binding site.<sup>3b</sup>

One may envision the antipicornaviral agents discussed in this paper binding to HRV-14 in one of two orientations either with the oxazoline ring in the "heel" of the binding pocket (the region near Leu<sup>106</sup> and Cys<sup>199</sup>) and the isoxazole moiety in the "toe" (the region near Phe<sup>186</sup>, Pro<sup>174</sup>, Val<sup>176</sup>, and Phe<sup>181</sup>) or in the reverse orientation. Compounds 5 and 6 bind in the former orientation shown in Figure 5. The remainder of the compounds in Table I bind in the latter fashion.<sup>5</sup>

Since the results of this study are entirely dependent on the biorelevant binding orientations, we have considered only the binding orientation of each antipicornaviral agent resulting from X-ray crystallography studies. Consequently, we are confident in the decision to consider only one of two possible orientations for each compound.

Studies are planned to investigate methods of predicting which of the two binding orientations an antipicornaviral agent would take in the binding pocket.

Finally, the question arises as to how these results impact on the mechanism of binding of these compounds to the viral capsid. Clearly, simply examining these molecules within the binding site without regard to how they arrive at their destination overlooks a vital aspect of the binding process. It has been shown that the on/off rates of several analogues are structure dependent.<sup>14</sup> The less bulky the molecule, the larger the on and off rates. Conversely, as bulk is added to the molecule, the on/off rates decrease. These results are explainable if one considers the conformational changes which occur at the binding site upon entry of the compounds. More energy is required to cause conformational changes with bulkier molecules and consequently the on rate is slower. However, once the molecule enters the binding site, the binding energy is now dependent upon hydrophobic interactions; hence the off rate is slower. There is also a view that gross conformational changes must occur in the virus capsid during the entry of a drug molecule. It is possible that the effects of charge and sterics at some intermediate point along the path of entry play an important role in deciding the overall activity of a compound.

The CoMFA studies which we have described support the conclusion that the binding of this class of compounds is due to hydrophobic interactions and, in addition, demonstrate the lack of an electronic effect.

## Experimental Section

Melting points were determined according to the USP procedure and are uncorrected. Where analysis are indicated only by the symbols of the elements, analytical results are within ±0.4% of the theoretical values. Analysis were performed by Galbraith Laboratories (Knoxville, TN). NMR spectra were determined on a JEOLFX-270 spectrophotometer, and all *J* values are in hertz.

4-[[[5-[3-(Hydroxymethyl)-5-isoxazolyl]pentyl]oxy]-3,5-dimethylbenzonitrile (14). A suspension of 8.5 g (42 mmol) of 5-(5-chloropentyl)-3-(hydroxymethyl)isoxazole (12),<sup>3b</sup> 5.89 g (40 mmol) of 3,5-dimethyl-4-hydroxybenzonitrile (13),<sup>15</sup> 7.0 g (42 mmol) of KI, and 20.7 g (150 mmol) of milled K<sub>2</sub>CO<sub>3</sub> in 100 mL of DMF was heated at 100 °C for 24 h. Upon cooling, the reaction mixture was partitioned between ether and water. The ethereal layer was washed with water and saturated brine then dried over MgSO<sub>4</sub> and filtered. The filtrate was concentrated in vacuo and the resulting brown oil (10.1 g) was subjected to MPLC (50 mm i.d., Kieselgel 60 column; 1:1 EtOAc/hexane), providing 6.5 g of 14 as a tan solid in 52% yield. Recrystallization from Et<sub>2</sub>O afforded 14 as a tan solid: mp 63–64 °C; <sup>1</sup>H NMR (d, 2 H, *J* =

(14) Fox, M. P.; McKinlay, M. A.; Diana, G. D.; Dutko, F. J. The Binding Affinities of Structurally Related Human Rhinovirus Capsid-Binding Compounds Correlate with Antiviral Activity. *Antimicrob. Agent Chemother.* **1991**, 35, 1040–1047.

(15) Fujio, M.; Mishima, M.; Tsuno, Y.; Yukawa, Y.; Takai, Y. Substituent Effect. V. NMR Chemical Shifts of Hydrogen-Bonding Hydroxyl Proton of Phenols in DMSO [dimethylsulfoxide]. *Bull. Chem. Soc. Jpn.* **1975**, 48, 2124–2127.

(16) Stewart, J. J. P. MOPAC version 5.0. *QCPE* **1989**, no. 455.

3.2 Hz), 3.79 (t, 2 H,  $J = 6.3$ ), 2.80 (d of d, 2 H,  $J = 7.5$  and 7.2), 2.40 (br, 1 H), 2.27 (s, 6 H), 1.81 (m, 4 H), 1.61 (m, 2 H). Anal. ( $C_{18}H_{22}N_2O_3$ ) C, H, N.

**5-[5-[2,6-Dimethyl-4-(1*H*-tetrazol-5-yl)phenoxy]pentyl]-3-isoxazolemethanol (15).** To a solution of 13.42 g (43 mmol) of 14 in 100 mL of DMF under nitrogen was added 3.25 g (50 mmol) of  $NaN_3$  and 0.3 g (6 mmol) of  $NH_4Cl$ . The mixture was shielded in a hood and heated to ca. 120 °C for 4 d. The resultant dark brown solution was concentrated in vacuo to one-half the original volume and poured into 250 mL of  $H_2O$ . The solution was shielded in a fume hood and chilled on ice while being acidified with 6 N HCl dropwise. A brown solid precipitated and was filtered and air-dried. Recrystallization from *i*-ProAc afforded 5.65 g of 15 as a tan solid in 78% yield: mp 127–130 °C;  $^1H$  NMR ( $DMSO-d_6$ )  $\delta$  7.72 (s, 2 H), 6.23 (s, 1 H), 5.40 (br, 1 H), 3.81 (t, 2 H,  $J = 6.0$ ), 3.35 (br, 1 H), 2.78 (d of d, 2 H,  $J = 6.9$  and 7.3). Anal. ( $C_{18}H_{23}N_5O_3$ ) C, H, N.

**5-[5-[2,6-Dimethyl-4-(2-methyl-5-tetrazolyl)phenoxy]pentyl]-3-isoxazolemethanol (16).** A suspension of 11.11 g (31 mmol) of 15, 5.5 g (40 mmol) of  $K_2CO_3$ , and 2 mL (50 mmol) of iodomethane in 100 mL of  $CH_3CN$  was stirred at room temperature overnight. The reaction mixture was concentrated in vacuo and partitioned between EtOAc and water. The organic layer was washed successively with water and saturated brine and then dried over  $MgSO_4$  and filtered. The resultant oil (11.08 g) was subjected to MPLC (50 mm i.d. Kieselgel 60 column; 6:4 EtOAc/hexane), providing 6.79 g of 16 in 59% yield. Recrystallization from ether afforded 16 as a tan solid: mp 82–83 °C;  $^1H$  NMR ( $CDCl_3$ )  $\delta$  7.79 (s, 2 H), 6.06 (s, 1 H), 4.73 (d, 2 H,  $J = 6.2$ ),  $\delta$  4.36 (s, 3 H), 3.81 (d of d, 2 H,  $J = 6.2$  and 6.4), 2.81 (d of d, 2 H,  $J = 7.2$  and 7.5), 2.36 (t, 1 H,  $J = 6.2$ ), 2.33 (s, 6 H), 1.83 (m, 4 H), 1.63 (m, 2 H). Anal. ( $C_{19}H_{25}N_5O_3$ ) C, H, N.

The 1-positional isomer of 16 was obtained in 27% yield: mp 65–68 °C;  $^1H$  NMR  $\delta$  7.384 (s, 2 H), 4.163 (s, 3 H).

**2-[[[5-[5-[2,6-Dimethyl-4-(2-methyl-5-tetrazolyl)phenoxy]pentyl]-3-isoxazolyl]methoxy]methoxy]ethanol (11).** A solution of 6.78 g (18 mmol) of 16, 15 g (70 mmol) of 2-(chloromethoxy)ethyl benzoate,<sup>9</sup> and 11 mL (63 mmol) of diisopropylethylamine in 75 mL of THF was magnetically stirred at room temperature for 48 h. The THF was removed in vacuo and the residue was partitioned between EtOAc and water. The organic layer was washed successively with  $H_2O$ , saturated  $NaHCO_3$ , and saturated brine. After drying, the solution was concentrated to dryness, providing an orange oil, which was flash chromatographed on silica gel with EtOAc and hexane (1:1). The oil was dissolved in a solution of 3.2 g (80 mmol) of NaOH in 400 mL of MeOH and left at room temperature for 0.5 h. The reaction was neutralized with AcOH and concentrated in vacuo, and the residue partitioned between EtOAc and water. The organic layer was washed successively with  $H_2O$  and saturated brine and then dried and concentrated. The resulting yellow oil (6.6 g) was subjected to MPLC (50 mm i.d. Kieselgel 60 column; 3:1 EtOAc/hexane), affording 4.1 g of 11 as a clear colorless oil in 51% yield:  $^1H$  NMR

( $CDCl_3$ )  $\delta$  7.78 (s, 2 H), 6.05 (s, 1 H), 4.80 (s, 2 H), 4.66 (s, 2 H), 4.36 (s, 3 H), 3.79 (t, 2 H,  $J = 6.3$ ), 3.72 (m, 4 H), 2.80 (d of d, 2 H,  $J = 7.6$  and 7.1), 1.81 (m, 4 H), 1.64 (m, 2 H). Anal. ( $C_{22}H_{31}N_5O_5$ ) C, H, N.

All of the studies described below were run on a Vax 11/785 using SYBYL version 5.2.

**CoMFA.** The eight compounds in Table I were used for this experiment. The structures of all of these compounds bound to HRV-14 had been individually solved and these conformations were used for this study in order to eliminate any questions about the "biorelevant" conformation. The structures were aligned by aligning the backbone atoms of the viral proteins within 20 Å from any atom of the compound. Thus the positioning of the drug molecules was obtained for this study without expressly overlapping any atoms of the drugs themselves.

The coordinates of the lower back corner and the upper front corner of a box that was used for the CoMFA analysis were determined by taking the coordinates of overlapped drug molecules and determining the minimum and maximum  $x$ ,  $y$ , and  $z$  values over the entire set of molecules. Two angstroms was added to each of the dimensions of this box (i.e. 1.0 Å to the minimum and maximum). The lower back corner was the minimum value (adjusted as above) and the upper front was the maximum value. These coordinates were -8, -8, -6 and 8, 2, 5, respectively. The grid size for the run was taken to be 1.0 Å. This generates a CoMFA table of approximately  $16 \times 20 \times 11$  (3520 points). The correlations which were sought were generated from Table II.

All charges on the molecule were calculated using the AM1 Hamiltonian without geometry optimization.<sup>18</sup> The charge on the probe atom (taken to have the van der Waals (VDW) radius of H) was taken to be 1.0.

The CoMFA was repeated for each reported run. First, a cross-validated run was performed to obtain the optimal number of components. These were routinely found to be one and consequently were insignificant. Then using this optimal value for the number of components, an identical run was performed without cross validation. The  $r^2$  value obtained from this run is the one reported, (see Table III). Finally, the entire exercise was repeated twice, once considering steric and electrostatic factors in the CoMFA and once considering only electrostatic factors (by explicitly setting the VDW table to zero for all atom types). No difference in the interpretation was evident and so only the first of these runs is reported.

**Acknowledgment.** We would like to extend our appreciation to Wendy Shave for providing the biological screening results, Tom Bailey for his chemical assistance, and Michael Rossmann, John Badger, Tom Smith, and Michael Chapman from Purdue University for the X-ray crystallography data. An author (A.M.T.) wishes to express his appreciation to Deborah A. Loughney for command level assistance in performing the CoMFA analysis.